Light: Science & Applications (2013) 2, e54; doi:10.1038/lsa.2013.10

www.nature.com/lsa

ORIGINAL ARTICLE

Radiation damping optical enhancement in cold atoms

Jin-Hui Wu[1], SAR Horsley[2], M Artoni[3,4] and GC La Rocca[5]

The typically tiny effect of radiation damping on a moving body can be amplified to a favorable extent by exploiting the sharp reflectivity slope at one edge of an optically induced stop-band in atoms loaded into an optical lattice. In this paper, this phenomenon is demonstrated for the periodically trapped and coherently driven cold ^{87}Rb atoms, where radiation damping might be much larger than that anticipated in previous proposals and become comparable with radiation pressure. Such an enhancement could be observed even at speeds of only a few meters per second with less than 1.0% absorption, making radiation damping experimentally accessible.
Light: Science & Applications (2013) **2,** e54; doi:10.1038/lsa.2013.10; published online 15 February 2013

Keywords: optically induced stop-band; ordered atomic structure; radiation damping; radiation pressure

INTRODUCTION

A body in motion relative to a light source experiences not only a light pressure but also a damping force that depends on its velocity, akin to a viscous friction.[1] Pressure is a result of the momentum exchange between light and matter due to photons scattering, while damping arises from the Doppler effect and opposes, for instance, the velocity of a moving mirror.[2] This velocity-dependent force damps mechanical oscillations at a rate of the order of $P=mc^2$, with P being the light power and m the mirror mass. Radiation damping could be used to control macroscopic moving objects or reversibly to implement precision motion sensing schemes. Gaining control over radiation damping forces is interesting in its own right.[3–6] However, this capability can also develop into a new approach to manage the dynamics of hybrid optomechanical atom-membrane interfaces,[7] where the motion of cold atoms is strongly coupled to the vibration of a micro-mechanical membrane.[8] Controlling the coherent motion of cold atoms *via* radiation damping, particularly if this control can be performed all-optically as we will demonstrate below, would permit substantial engineering of the mechanical oscillator, including the quantum-limited read-out of its position[9–12] and the efficient exchange of quantum states among light, the oscillator and cold atoms.[13]

However, for ordinary velocities and a light power that is not too large to destroy the mirror, radiation damping is usually several orders of magnitude smaller than the pressure and, hence, particularly difficult to detect, even for the smallest diffraction-limited mirrors of $m\approx10^{-12}$ g.[14–16] With such a small figure, radiation damping can hardly be of any practical use at variance, e.g., with radiation pressure that is routinely employed to cool atoms.[17] Methods to enhance such a typically tiny damping are now being sought for. This enhancement is performed by exploiting the sharp optical response near one edge of the photonic stop-band in a dielectric Bragg mirror[15] or in a one-dimensional (1D) ordered structure of cold ^{87}Rb atoms.[18] In the latter case, this enhancement hinges on the formation of stop-bands near an atomic resonance in a periodic atomic structure, a subject that is relatively unexplored.[19–24] Only very recent experiments have reported quite sharp reflectivity profiles in this regime.[25,26]

Hence, we propose here a new mechanism to achieve a large radiation damping effect in a 1D atomic photonic crystal. The enhancement is found to occur around a narrow stop-band opening up in the cold confined ^{87}Rb atoms when driven into a Λ configuration[27] of levels by a pump beam (cf. Figure 1) that allows for an efficient all-optical (external) control. The expected enhancement occurs in the Autler–Townes (AT) splitting regime and arises from the ultrahigh sensitivity of reflectivity (transmissivity) near such an optically induced stop-band. Consequently, the enhancement can be controlled on demand by changing the pump intensity and frequency. In a cold sample of density 6.0×10^{12} cm^{-3}, e.g., for atoms sloshing within the confining optical potential at characteristic velocities (about 1.0 m s^{-1}), the radiation damping force may become so strong as to compare with the radiation pressure. Controllable damping enhancement of various orders of magnitude, with a concomitant large suppression of absorption, makes this proposal a remarkable improvement over previous ones[15,18] and a viable option for the observation of radiation damping effects.

MATERIALS AND METHODS

Our ensemble of cold ^{87}Rb atoms is loaded into an optical lattice of period a formed by retro-reflecting a light beam of wavelength $\lambda_o=2a$ (Figure 1). In each period of such a dipole trap, the confined atoms occupy a small region $d<<a$ with a homogeneous volume density N_0. This periodic 1D index modulation will cause pronounced photonic stop-bands as expected.[25] We use the transfer matrix formalism to describe the propagation of a probe field of frequency ω_p through such an atomic stack, referring to Ref. 22 for a detailed description

[1]College of Physics, Jilin University, Changchun 130012, China; [2]Electromagnetic and Acoustic Materials Group, Department of Physics and Astronomy, University of Exeter, Stocker Road, Exeter, EX4 4QL, UK; [3]European Laboratory for Nonlinear Spectroscopy, Sesto Fiorentino, Italy; [4]Department of Physics and Chemistry of Materials & CNR-IDASC Sensor Lab, Brescia University, Brescia, Italy and [5]Scuola Normale Superiore and CNISM, Pisa, Italy
Correspondence: Professor JH Wu, College of Physics, Jilin University, Changchun 130012, China
E-mail: jhwu@jlu.edu.cn
Received 27 July 2012; revised 28 October 2012; accepted 29 October 2012

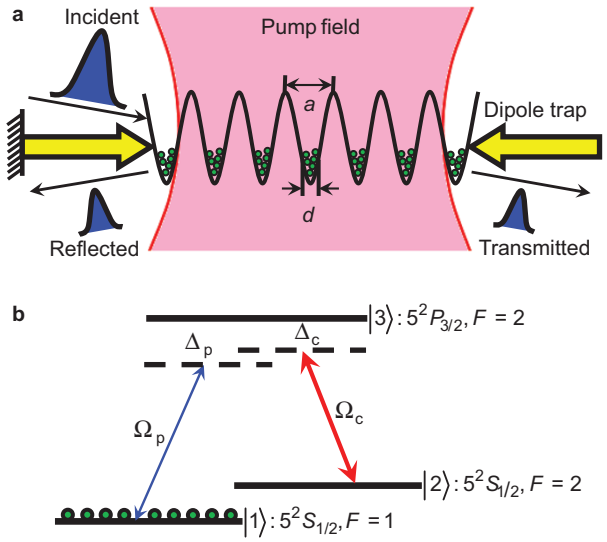

Figure 1 (**a**) Atomic Bragg mirror obtained by loading cold ^{87}Rb atoms into an optical lattice formed by retro-reflecting a laser beam of wavelength λ_o that is far-detuned from relevant atomic resonances (dipole trap). The confined atoms arrange themselves into a 1D chain of pancake-shaped layers with an average thickness d and are located at the standing-wave antinodes of period $a=\lambda_o/2$. Such an ordered atomic structure can be set to move coherently inside the lattice.[28,29] When a weak probe pulse impinges from the left, the moving Bragg mirror experiences a (viscous) friction force that depends on its velocity v and can be all-optically controlled through the frequency and intensity of an external pump. (**b**) The slightly detuned probe (Ω_p) and pump (Ω_c) fields drive all the confined cold atoms into a three-level Λ configuration. The three states correspond to the hyperfine split levels of the D_2 line in ^{87}Rb.

of this formalism in a similar context. From the frequency-dependent transfer matrix $M(\omega_p)$ for a single period and with the use of the Bloch theorem, we obtain the following dispersion relation:

$$e^{2i\kappa a} - Tr\left[M(\omega_p)\right]e^{i\kappa a} + 1 = 0 \qquad (1)$$

whose solutions yield the complex Bloch wave vector $\kappa=\kappa'+i\kappa''$. The refractive index associated with the collection of cold trapped atoms, $n(\omega_p)=\sqrt{1+\chi(\omega_p)}$ that enters $M(\omega_p)$ is obtained from:

$$\chi(\omega_p) = \frac{N_0\mu_{13}^2}{2\varepsilon_0\hbar}\frac{\gamma_{12}-i(\Delta_p-\Delta_c)}{\left[\gamma_{12}-i(\Delta_p-\Delta_c)\right](\gamma_{13}-i\Delta_p)+\Omega_c^2} \qquad (2)$$

where γ_{12} (γ_{13}) is the dephasing rate of the spin (optical) coherence ρ_{12} (ρ_{13}), $\Delta_p=\omega_p-\omega_{31}$ ($\Delta_c=\omega_c-\omega_{32}$) is the probe (pump) detuning relative to transition $|1\rangle\leftrightarrow|2\rangle$ ($|1\rangle\leftrightarrow|3\rangle$), and μ_{13} denotes the relevant electric-dipole moment. Here, we assume that the cold ^{87}Rb atoms are driven into a three-level Λ-type configuration[27] on the D_2 line by a probe of Rabi frequency Ω_p traveling in the x-direction and a pump of Rabi frequency Ω_c traveling in the y- (or z-) direction (Figure 1). Note that the probe field may have a small angle of incidence (e.g., $\theta\approx2^0$) in the x-direction of an oscillating atomic lattice.[22,25] The dressed susceptibility in Equation (1) holds in the limit of a weak probe ($\Omega_p<<\Omega_c$), within the rotating-wave and electric-dipole approximations. In particular, Equation (1) recovers the case of a single absorption line when $\Omega_c\to0$, but implies a narrow electromagnetically induced transparency (EIT) window near the probe resonance when $\Omega_c\leqslant\gamma_{13}$ due to the quantum destructive interference between two dressed-state transitions. However, for $\Omega_c>>\gamma_{13}$, the dressed susceptibility evolves into that for two well-separated AT split levels with the quantum destructive interference becoming unimportant.

Solving Equation (1) for κ' and κ'' as a function of $\omega_p(\Delta_p)$ yields photonic band-gaps that appear at the boundary of the first Brillouin zone ($\kappa'=\pi/a$);[22] these band gaps are shown in the left and right panels of Figure 2, respectively, in the presence or absence of the pump. We recall that in a non-resonant multilayer stack, as for a standard distributed Bragg reflector,[15] a single stop-band opens up near the Bragg frequency; conversely, in the presence of a resonant absorption line near the Bragg frequency,[18] two stop-bands will arise from the interplay between the polaritonic gap due to the resonance and the Bragg gap due to the periodic index modulation. The latter case is featured in Figure 2b and 2d where, for a susceptibility $\chi(\omega_p)$ in the case without the pump ($\Omega_c=0$), two wide stop-bands open up in negative and positive detuning regions near a single absorption line. However, when the pump is on ($\Omega_c\neq0$), as illustrated in Figure 2a and 2c, a third narrow stop-band arises[24,26] and fits between the two wide ones separated by the AT split absorption lines.

In the following, we focus on this additional stop-band by applying a strong pump to attain AT splitting beyond the EIT regime.[27] The width and position of this narrow stop-band can be manipulated through the modulation of pump frequency and intensity, which then allows us to efficiently control the optomechanical properties of our atomic multilayer. The most relevant damping effects we address here occur in the steepest region of the reflectivity and transmissivity profiles near one edge of this third stop-band, where absorption is significantly suppressed. This result is particularly relevant in that the excited absorption and spontaneous emission cycles may randomize the atomic motion and hamper the experimental observation of radiation damping.[30–34] However, the actual values of the spin dephasing rate γ_{12} of cold atoms confined in the optical lattice[26] do not play a crucial role in determining the optical response as long as $\Omega_c>>\gamma_{13}>>\gamma_{12}$, and our results do not significantly change for the range of values 1.0 kHz$<\gamma_{12}<$100 kHz.

In a typical experimental situation, it is no longer adequate to only obtain the band dispersion *via* Equation (1). For a finite sample, we would need to compute the reflectivity R, transmissivity T and absorption $A=1-R-T$ from the transfer matrix M_N of the entire stack

$$M_N = M^N = \frac{\sin N\kappa a}{\sin\kappa a}M - \frac{\sin(N-1)\kappa a}{\sin\kappa a}I \qquad (3)$$

where I is the unity matrix and N is the number of primitive cells ($L=Na$). From Equation (3), we compute the probe reflectivity $R=\left|M_{N(12)}/M_{N(22)}\right|^2$ and transmissivity $T=\left|1/M_{N(22)}\right|^2$ for a sample of density $N_0=6.0\times10^{12}$ cm^{-3} and length $L=2.0$ cm; relevant results are plotted in Figure 2 in the three stop-bands region near resonance. The probe reflectivity behaves quite differently within each stop-band, which may be attributed to the fact that κ'', a measure of the extinction rate of evanescent waves, has very different values within these stop-bands. The central narrow stop-band, at variance with the other two, exhibits a much steeper optical response at the edge near atomic resonance, where $R(\omega_p)$ sharply drops to zero from a homogeneous 100% reflectivity plateau as illustrated in Figure 2e. We further compare in Figure 2f the reflectivity (transmissivity) when the pump is off. In the absence of the central stop-band, we observe a much milder frequency-sensitivity around resonance yet accompanied by a remarkable absorption.

RESULTS AND DISCUSSION

The overall light force experienced by a cold sample of ^{87}Rb atoms oscillating in a 1D optical lattice is obtained by first computing the

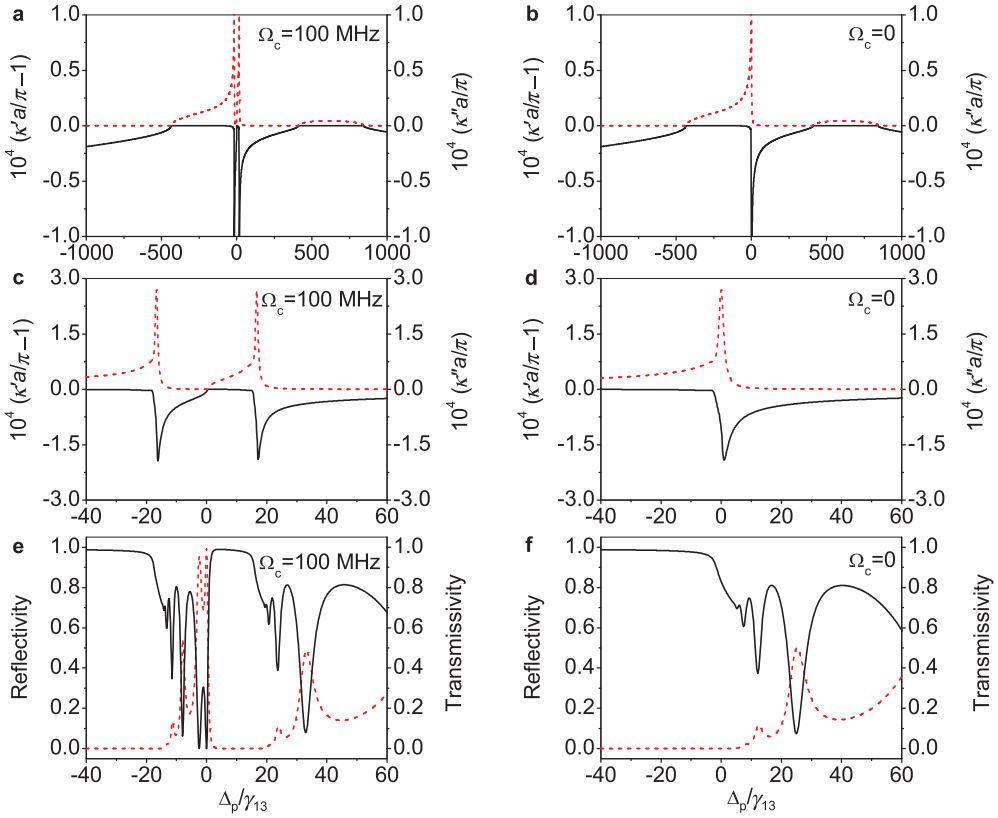

Figure 2 Real (black-solid) and imaginary (red-dashed) parts of the Bloch wave vector κ as a function of probe detuning Δ_p for an infinite periodic structure of cold ^{87}Rb atoms as determined from Equations (1)–(2) with (**a**) and without (**b**) the pump. The relevant parameters are γ_{13}=6.0 MHz, Δ_c=0, N_0=6.0×10^{12} cm^{-3}, μ_{13}=1.5×10^{-29} C m, λ_p=780.792 nm, a=780.787/2 nm and d=a/20. (**c**) and (**d**) are enlargements of (**a**) and (**b**), respectively, in the resonance region. (**e**) and (**f**) present the reflectivity (black-solid) and transmissivity (red-dashed) profiles corresponding to (**c**) and (**d**), respectively, for a L=2.0 cm long periodic structure of cold ^{87}Rb atoms as determined from Equation (3).

transfer rate of the four-momentum dP^μ/dt in the atoms' rest frame with the help of a Maxwell stress tensor. Upon Lorentz-transforming to the lab (primed) frame, where the atoms move with a velocity v along x, the relevant component of the average four-force $\langle dP^\mu/dt\rangle'$ is:[18]

$$\left\langle \frac{dP^x}{dt} \right\rangle' = \frac{\eta^2 P'}{c} \frac{\wp^x\left(\eta\omega_p'\right)}{\sqrt{1-(v/c)^2}} \approx \frac{P'}{c}\left[F_{(0)}^x - \frac{v}{c}F_{(1)}^x\right] \qquad (4)$$

where $\eta=\sqrt{(1-v/c)/(1+v/c)}$ and $\omega_p'=\omega_p/\eta$ result from the Lorentz transformation and $\wp^x(\eta\omega_p')$ is the force in units of the incident light mean power (P') over the speed of light (c). The momentum transfer rate and hence $\wp^x(\eta\omega_p')$ depend on the atoms' velocity v through the reflectivity and transmissivity in a complicated manner. However, for velocity ranges typical of experiments involving cold atoms in moving optical lattices, one has $\eta\approx1-v/c$ such that it is viable to expand $R\left(\eta\omega_p'\right)$ and $T\left(\eta\omega_p'\right)$, which appear in $\wp^x(\eta\omega_p')$. To the first order in v/c, one arrives at the simplified expression on the right-hand side of Equation (4), where $F_{(0)}^x=1+R\left(\omega_p'\right)-T\left(\omega_p'\right)$ and $F_{(1)}^x=1+3R\left(\omega_p'\right)-T\left(\omega_p'\right)+\omega_p'\left[\partial R\left(\omega_p'\right)\Big/\partial\omega_p'-\partial T\left(\omega_p'\right)\Big/\partial\omega_p'\right]$ are, respectively, the velocity-independent and velocity-dependent force components. This expansion is valid provided that the Doppler shift $(v/c)\omega_p'$ is smaller than the frequency range over which $R\left(\omega_p'\right)$ sharply rises to unity at the stop-band edge. Such a frequency range is approximately $1.5\gamma_{13}$ in Figure 2e, but becomes four times as much in Figure 4a.

It follows from Equation (4) that, for a lossless ($R=1-T$) and non-dispersive ($\partial R\Big/\partial\omega_p'=\partial T\Big/\partial\omega_p'=0$) medium, the velocity-independent term reduces to the pressure force $+2R\left(\omega_p'\right)P'\Big/c$, while the velocity-dependent term reduces to the damping force $-4R\left(\omega_p'\right)P'v\Big/c^2$. The latter is much smaller than the former, which makes the damping force difficult to observe for practical lattice velocities v and light powers P. To have $F_{(0)}^x\approx(v/c)F_{(1)}^x$ and attain a large enough radiation damping, we should try to find a highly dispersive medium with $\partial R\Big/\partial\omega_p'-\partial T\Big/\partial\omega_p'\approx c/\left(v\omega_p'\right)$ accompanied by negligible absorption. This objective can be achieved with cold ^{87}Rb atoms loaded into an optical lattice and driven into the Λ configuration as discussed above.

Another case may be relevant when the probe field is a Gaussian light pulse (containing $\overline{N}>>1$ photons) instead of a monochromatic plane light wave. In this case, we can verify how the momentum transfer from a light pulse to a periodic atomic structure depends on its oscillating velocity (i.e., the Doppler shift). Relevant results will be used as direct evidence to determine whether the damping force is comparable to or even larger than the light pressure. The net momentum ΔP^x imparted in the lab frame by a light pulse can be obtained by integrating the scaled force $\wp\left(\eta\omega_p'\right)$ over the pulse (normalized) frequency distribution $f\left(\omega_p'\right)$.

The main panels of Figure 3a and 3c indicate a (normalized) damping force $F_{(1)}^x\approx+9.7\times10^8$ and absorption $A\approx0.3\%$ near $\Delta_p=0.5\gamma_{13}$

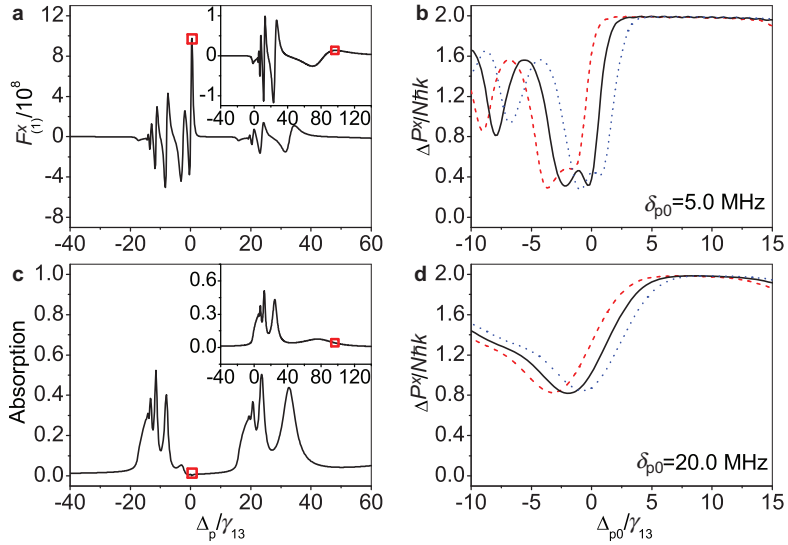

Figure 3 Normalized damping force (**a**) and absorption (**c**) as a function of probe detuning Δ_p for a 2.0-cm long periodic structure of cold ^{87}Rb atoms in the presence of the pump. The insets show the corresponding force and absorption when the pump is off. The relevant parameters are the same as those in Figure 2. Normalized momentum transfer from a Gaussian light pulse to the same atomic structure of cold ^{87}Rb as a function of central-frequency detuning Δ_{p0} with pulse width δ_{p0}=5.0 MHz (**b**); δ_{p0}=20.0 MHz (**d**). The black-solid, red-dashed and blue-dotted curves refer to velocities v=0.0, +6.0 and −6.0 m s^{-1}, respectively.

(denoted by a red square) in the resonance region when a pump with Ω_c=100 MHz is on. Conversely, in the insets of Figure 3a and 3c where the pump is off (Ω_c=0), we have $F^x_{(1)} \approx +1.3\times10^7$ and A≈7.6% near Δ_p=97.0γ_{13} (denoted by a red square) away from resonance; otherwise, the absorption would be too large.[18] This result clearly indicates that the damping force can be further amplified 70 times and the probe absorption can be further suppressed 25 times when working with the central stop-band rather than the other two. When shorter samples are used (L=0.5 cm), the probe reflectivity and transmissivity are not as steep as before; however, we still obtain rather favorable results with $F^x_{(1)} \approx +2.3\times10^8$ and A≈0.6% near Δ_p=1.5γ_{13} at one edge of the optically induced stop-band as demonstrated separately in Figure 4. It is important to note that the damping force $[\propto (v/c)F^x_{(1)}]$ may be enhanced to be comparable with the pressure force $[\propto F^0_{(1)}]$ for v as small as several tens of cm s^{-1}, making the tiny optomechanical effect of radiation damping accessible to potential experiments. Note that larger velocities are considered in the more relevant case of a light pulse, such as in Figure 3b and 3d where the four-force component $\langle dP^x/dt\rangle'$ is computed by the exact expression of Equation (4) rather than the approximate expansion following it.

Figure 3b and 3d shows the momentum transfer ΔP^x, in units of the incident light total momentum $\overline{N}\hbar k$, for a pulse with a Gaussian frequency distribution $f\left(\omega'_p\right) = \left(\sqrt{\pi}\delta_{p0}\right)^{-1}\exp\left[-\left(\omega'_p-\omega_{p0}\right)^2\Big/\delta^2_{p0}\right]$ centered at ω_{p0}. This quantity depends critically on the lattice velocity v when the pulse width δ_{p0} is small enough that it doesn't extend

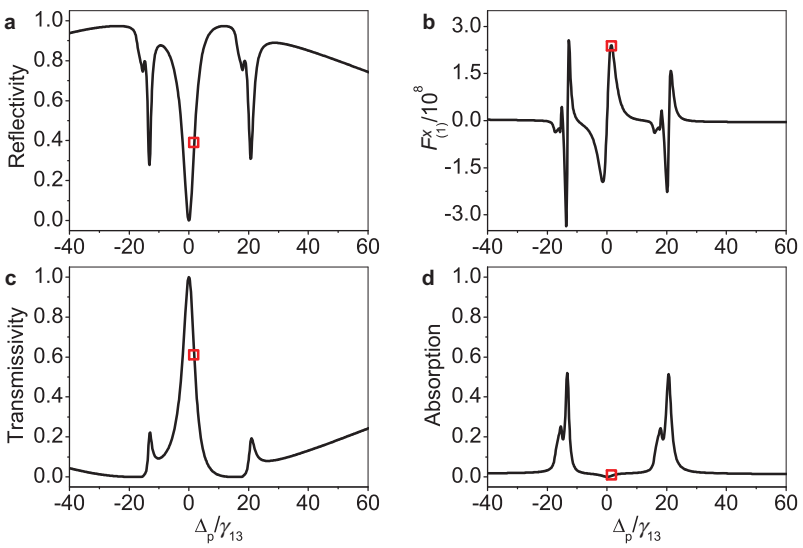

Figure 4 Reflectivity (**a**), normalized damping force (**b**), transmissivity (**c**) and absorption (**d**) as a function of probe detuning Δ_p for a shorter periodic structure of cold ^{87}Rb atoms in the presence of the pump. The relevant parameters are the same as in Figure 2 except L=0.5 cm.

beyond the steep edge of the stop-band. In numerical calculations, we have defined $\Delta_{p0}=\omega_{p0}-\omega_{31}$ as the central-frequency detuning of the light pulse relative to the probe resonance. From Figure 3b, we can see that for a negative (positive) velocity $\upsilon=-6.0$ m s^{-1} ($\upsilon=+6.0$ m s^{-1}), the normalized momentum transfer is increased from 0.38 to 1.62 (decreased from 1.70 to 0.66) at $\Delta_{p0}\approx 0.0\gamma_{13}$ ($\Delta_{p0}\approx 1.33\gamma_{13}$) compared with that attained for $\upsilon=0.0$ m s^{-1}. This result indicates that the radiation damping will significantly enhance (weaken) the radiation pressure when a medium moves toward (away from) the light pulse and, thus, always tends to prevent the motion of this medium. Figure 3d further demonstrates that an increase of the pulse width will lead to a decrease of the sensitivity of momentum transfer on the medium velocity.

CONCLUSIONS

In summary, we have investigated the steady optical response of a periodic structure of cold ^{87}Rb atoms driven into the Λ configuration and discussed its potential application for the enhancement of typically tiny radiation damping forces. This periodic atomic structure has three photonic stop-bands of high reflectivity near the probe resonance, among which the central narrower one is optically induced by a pump field. At one edge of this dynamically controlled stop-band, the reflectivity is very sensitive to the probe frequency yet accompanied by little absorption. This peculiar property has been exploited to obtain a greatly amplified effect of radiation damping, accessible to experiments when an optical lattice oscillates at a velocity of approximately 1.0 m s^{-1}. Although our treatment concerns a semiclassical atomic velocity υ, the predicted radiation damping would also affect the atomic motion even in a fully quantum regime.[13,35] Finally, our scheme does not rely on any concept unique to atoms. Well-developed stop-bands can also be optically induced, e.g., in a diamond crystal doped with N–V color centers,[36] where radiation damping enhancement may then be anticipated to occur.

ACKNOWLEDGMENTS

This work is supported by the National Natural Science Foundation of China (11104112), the National Basic Research Program of China (2011CB921603), the CRUI-British Council 2011 Exchange Program and the Fondo di Ateneo of the Brescia University. JH Wu would also like to acknowledge the hospitality of Scuola Normale Superiore in Pisa.

1 Braginski VB, Makunin AB. Ponderomotive effects of electromagnetic radiation. *Sov Phys JETP* 1967; **25**: 653–655.
2 Matsko AB, Zibova EA, Vyatchanin SP. The value of the force of radiative friction. *Opt Commun* 1996; **131**: 107–113.
3 Borgnis FE. Acoustic radiation pressure of plane compressional waves. *Rev Mod Phys* 1953; **25**: 653–664.
4 Ashkin A. Forces of a single-beam gradient laser trap on a dielectric sphere in the ray optics regime. *Biophys J* 1992; **61**: 569–582.
5 Arcizet O, Cohadon PF, Briant T, Pinard M, Heidmann A. Radiation-pressure cooling and optomechanical instability of a micromirror. *Nature* 2006; **444**: 71–74.
6 Horsley SA, Artoni M, La Rocca GC. Radiation pressure on a moving body: beyond the Doppler effect. *J Opt Soc Am B* 2012; **29**: 3136–3140.
7 Schliesser A, Kippenberg TJ. Viewpoint: hybrid atom-optomechanics. *Physics* 2011; **4**: 97.
8 Camerer S, Korppi M, Jockel A, Hunger D, Hansch TW *et al*. Realization of an optomechanical interface between ultracold atoms and a membrane. *Phys Rev Lett* 2011; **107**: 223001.
9 Safavi-Naeini AH, Chan J, Hill JT, Alegre TP, Krause A *et al*. Observation of quantum motion of a nanomechanical resonator. *Phys Rev Lett* 2012; **108**: 033602.
10 Schliesser A, Arcizet O, Riviere R, Anetsberger G, Kippenberg TJ. Resolved-sideband cooling and position measurement of a micromechanical oscillator close to the Heisenberg uncertainty limit. *Nat Phys* 2009; **5**: 509–514.
11 Teufel JD, Donner T, Castellanos-Beltran MA, Harlow JW, Lehnert KW. Nanomechanical motion measured with an imprecision below that at the standard quantum limit. *Nat Nanotech* 2009; **4**: 820–823.
12 O'Connell AD, Hofheinz M, Ansmann M, Bialczak RC, Lenander M *et al*. Quantum ground state and single-photon control of a mechanical resonator. *Nature* 2010; **464**: 697–703.
13 Marquardt F, Clerk AA, Girvin SM. Quantum theory of optomechanical cooling. *J Mod Opt* 2008; **55**: 3329–3338.
14 Favero I, Metzger C, Camerer S, Konig D, Lorentz H *et al*. Optical cooling of a micromirror of wavelength size. *Appl Phys Lett* 2007; **90**: 104101.
15 Karrai K, Favero I, Metzger C. Doppler optomechanics of a photonic crystal. *Phys Rev Lett* 2008; **100**: 240801.
16 Marquardt F, Girvin SM. Trends: optomechanics. *Physics* 2009; **2**: 40.
17 Phillips WD, Metcalf HF. Cooling and trapping atoms. *Sci Am* 1987; **256**: 36–42.
18 Horsley SA, Artoni M, La Rocca GC. Radiation damping in atomic photonic crystals. *Phys Rev Lett* 2011; **107**: 043602.
19 Deutsch IH, Spreeuw RJ, Rolston SL, Phillips WD. Photonic band gaps in optical lattices. *Phys Rev A* 1995; **52**: 1394–1410.
20 van Coevorden DV, Sprik R, Tip A, Lagendijk A. Photonic band structure of atomic lattices. *Phys Rev Lett* 1996; **77**: 2412–2415.
21 Andre A, Lukin MD. Manipulating light pulses *via* dynamically controlled photonic band gap. *Phys Rev Lett* 2002; **89**: 143602.
22 Artoni M, La Rocca GC, Bassani F. Resonantly absorbing one-dimensional photonic crystals. *Phys Rev E* 2005; **72**: 046604.
23 Artoni M, La Rocca GC. Optically tunable photonic stop bands in homogeneous absorbing media. *Phys Rev Lett* 2006; **96**: 073905.
24 Petrosyan D. Tunable photonic band gaps with coherently driven atoms in optical lattices. *Phys Rev A* 2007; **76**: 053823.
25 Schilke A, Zimmermann C, Courteille PW, Guerin W. Photonic band gaps in one-dimensionally ordered cold atomic vapors. *Phys Rev Lett* 2011; **106**: 223903.
26 Schilke A, Zimmermann C, Guerin W. Photonic properties of one-dimensionally-ordered cold atomic vapors under conditions of electromagnetically induced transparency. *Phys Rev A* 2012; **86**: 023809.
27 Fleischhauer M, Imamoglu A, Marangos JP. Electromagnetically induced transparency: optics in coherent media. *Rev Mod Phys* 2005; **77**: 633–673.
28 Gorlitz A, Weidemuller M, Hansch TW, Hemmerich A. Observing the position spread of atomic wave packets. *Phys Rev Lett* 1997; **78**: 2096–2099.
29 Raithel G, Phillips WD, Rolston SL. Collapse and revivals of wave packets in optical lattices. *Phys Rev Lett* 1998; **81**: 3615–3618.
30 Marzlin KP, Zhang WP. Photonic band gaps and defect states induced by excitations of Bose–Einstein condensates in optical lattices. *Phys Rev A* 1999; **59**: 2982–2989.
31 Morsch O, Muller JH, Cristiani M, Ciampini D, Arimondo E. Bloch oscillation and mean-field effects of Bose–Einstein condensates in 1D optical lattices. *Phys Rev Lett* 2001; **87**: 140402.
32 Fort C, Cataliotti FS, Fallani L, Ferlaino F, Maddaloni P *et al*. Collective excitation of a trapped Bose–Einstein condensate in the presence of a 1D optical lattice. *Phys Rev Lett* 2003; **90**: 140405.
33 Murch KW, Moore KL, Gupta S, Stamper-Kurn DM. Observation of quantum-measurement backaction with an ultracold atomic gas. *Nat Phys* 2008; **4**: 561–564.
34 Rist S, Menotti C, Morigi G. Light scattering by ultracold atoms in an optical lattice. *Phys Rev A* 2010; **81**: 013404.
35 Aspelmeyer M, Meystre P, Schwab K. Quantum optomechanics. *Phys Today* 2012; **65**: 29–35.
36 Wu JH, La Rocca GC, Artoni M. Controlled light-pulse propagation in driven color centers in diamond. *Phys Rev B* 2008; **77**: 113106.